that aggregation of the dye is not necessary. The order of magnitude difference in the Kerr constant dispersions in the 5000-A region suggests that the intercalated structure is transformed into the surface bound structure as the relative amount of dye is increased. The older ORD results of Neville and Bradley[7] also show this same effect as the shorter wavelength dispersion grows at the expense of the longer wavelength one as the amount of dye is increased. It is quite possible that the recent suggestion concerning partial intercalation[24] is correct and that, as the surface sites are filled, the intercalated dye is removed from between the bases to form the dye aggregate.

Acknowledgment. The authors wish to thank Mr. John H. Smith for technical assistance and Professor N. Davidson for helpful discussions and the loan of the thesis of H. Ohlenbusch.

(24) N. J. Pritchard, A. Blake, and A. R. Peacocke, *Nature*, **212**, 1360 (1966).

Coalescence of Mercury Droplets in Aqueous Solutions, with Special Reference to the Examination of Double-Layer Interaction

by Shinnosuke Usui, Taro Yamasaki,

Research Institute of Mineral Dressing and Metallurgy, Tohoku University, Nagamachi, Sendai, Japan

and Junzo Shimoiizaka

Department of Mining and Mineral Engineering, Tohoku University, Aobayama, Sendai, Japan
(Received February 9, 1967)

The coalescence of mercury droplets in aqueous KF solution at concentrations of 10^{-3} to 10^{-2} M was examined by means of twin dropping mercury electrodes. From the critical potentials for the coalescence in the symmetrical case where two mercury droplets were equally charged, 1.2×10^{-12} was obtained as a reliable value of the Hamaker constant for mercury in water. The critical potentials in the asymmetrical case where two mercury droplets were unequally charged were also determined. The agreement between the theoretical and experimental values showed the validity of the Derjaguin–Landau–Verwey–Overbeek theory and the dissimilar double-layer interaction theory. The behavior of the coalescence in the presence of specific adsorption of I^- ions was interpreted qualitatively in terms of the potential of the outer Helmholtz plane at the mercury–solution interface.

Introduction

The coagulation of colloidal dispersion has been discussed by the Derjaguin–Landau–Verwey–Overbeek (DLVO) theory which is based on the electrical repulsion and the long-range London–van der Waals attraction between particles.[1] Experimental verifications of this theory have been attempted on various sols. However, the results have been discussed by using an ambiguous quantity like the electrokinetic ζ potential.

(1) E. J. W. Verwey and J. Th. G. Overbeek, "Theory of the Stability of Lyophobic Colloids," Elsevier Publishing Co., Amsterdam, 1948.

The van der Waals attraction is usually obtained from the coagulation experiments by estimating the residual interaction after allowance has been made for the electrical forces. The Hamaker constants so derived are dependent on the choice of the potential, and reliable values of the Hamaker constant in a simple system have been unavailable. Furthermore, many of the investigations have dealt almost exclusively with the case where particles are equally charged, and few experimental studies have been conducted on the coagulation of unequally charged particles. The theory of the dissimilar double-layer interaction and the theory of heterocoagulation have already been presented by Derjaguin,[2] Bierman,[3] Devereux and de Bruyn,[4] and Hogg, Healy, and Fuerstenau.[5] The difficulty associated with the experimental verification of these theories is believed to lie in the method under such conditions that the interfacial potential of particles and electrolyte concentration can be freely changed, because the interfacial potential of particles is uniquely determined when the system of particle–electrolyte solution is specified.

In connection with these problems, an interesting experiment was undertaken by Watanabe and Gotoh.[6] They studied the coalescence of mercury droplets by means of twin electrodes and demonstrated that the coalescence of mercury droplets was substantially the same as the coagulation of hydrophobic colloid particles and was interpreted quantitatively by the DLVO theory. However, their result lacked in the quantitative treatment of the difference between the rational potential of the electrode and the Stern potential. The twin dropping mercury electrode technique is characterized by the fact that the potential of mercury is controlled to any desired one if a mercury–electrolyte solution interface is in a polarized state.

The purpose of the present study is to examine the DLVO theory in terms of well-defined quantities, *i.e.*, the rational potential of the electrode and the potential of the outer Helmholtz plane of mercury, and to investigate the theory of dissimilar double-layer interaction through the coalescence of mercury droplets by using the twin electrode technique.

Experimental Section

Devices and Materials. The twin electrodes used in this study are shown in Figure 1a and are virtually identical with those used by Watanabe and Gotoh,[6] some modifications being that two potentiometers (P_1 and P_2) were employed to polarize the mercury droplets and a 1 *N* calomel electrode (nce) was used as a reference electrode. Another important improvement was in capillary tip design as shown in Figure 1b,

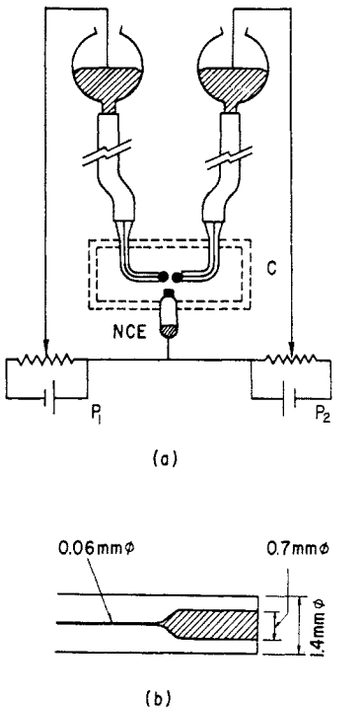

Figure 1. (a) Twin dropping mercury electrodes: P_1, P_2, potentiometer; NCE, 1 *N* calomel electrode; C, plastic cell. (b) Schematic of glass capillary tip in cross-section.

which was indispensable to obtaining reliable and reproducible results. The coalescence experiments were carried out at the flowing rate of mercury of about 1 mg/sec during the course of these investigations.

The plastic cell has a thermostating jacket through which water may circulate from a constant-temperature (25°) source. The capacity of the cell is about 100 ml. Test solutions were deoxygenated by argon bubbling, and measurements were made under the atmospheric condition of an argon stream. The apparatus used for differential capacity measurements was essentially identical with that used by Grahame[7] and is shown in Figure 2. The frequency utilized was 100 cps.

KF was selected as an electrolyte because the specific adsorption of F^- ion at the mercury–solution interface is thought to be negligible. KI was also used for comparison because of the strong tendency of specific ad-

(2) B. V. Derjaguin, *Discussions Faraday Soc.*, **18**, 85 (1954).

(3) A. Bierman, *J. Colloid Sci.*, **10**, 231 (1955).

(4) O. F. Devereux and P. L. de Bruyn, "Interaction of Plane-parallel Double Layers," MIT Press, Cambridge, Mass., 1963.

(5) R. Hogg, T. W. Healy, and D. W. Fuerstenau, *Trans. Faraday Soc.*, **62**, 1638 (1966).

(6) A. Watanabe and R. Gotoh, *Kolloid-Z.*, **191**, 36 (1963).

(7) D. C. Grahame, *J. Am. Chem. Soc.*, **71**, 2975 (1949).

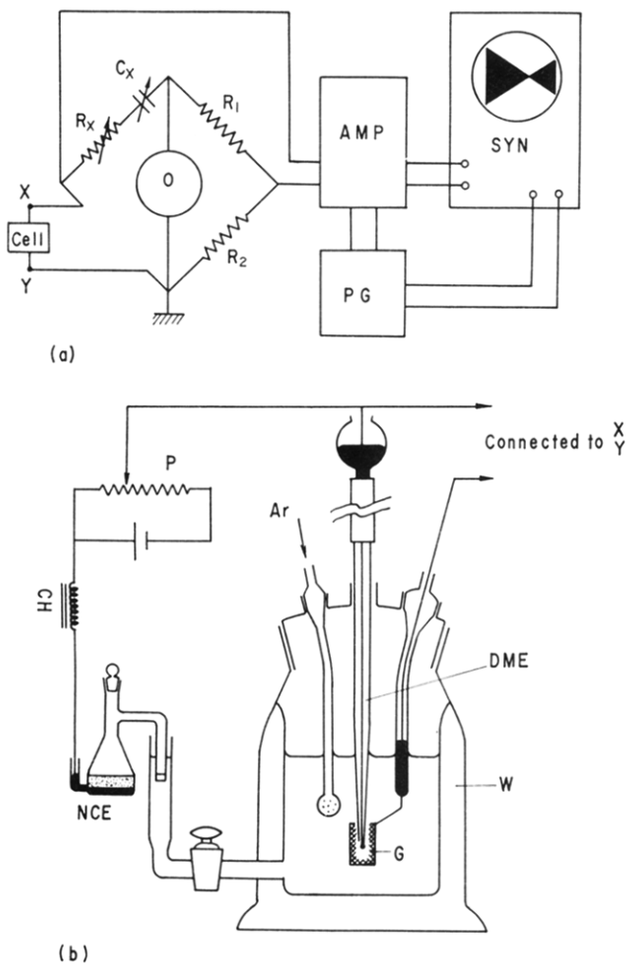

Figure 2. (a) Block diagram of apparatus for differential capacity measurement: R_x, standard variable resistor; C_x, standard variable capacitor; R_1, R_2, resistors; O, twin T oscillator; AMP, twin T differential amplifier; PG, pulse generator; SYN, synchroscope. (b) Schematic of cell for differential capacity measurement: P, potentiometer; CH, choke coil (150 henrys); NCE, 1 *N* calomel electrode; DME, dropping mercury electrode; G, Pt gauze (counterelectrode); W, circulating water jacket.

sorption of I^- ion. Guaranteed grade KF and KI were further recrystallized from conductivity water. The conductivity water was obtained by redistillation from alkali permanganate solution, followed by distillation without the reagent, the specific conductivity of which was less than 1×10^{-6} ohm^{-1} cm^{-1}. The cleaned air was led into high-purity mercury (99.9999%) for 3 days, and then the mercury was washed well with dilute HNO_3 solution and distilled water, dried, and finally distilled twice *in vacuo*.

Procedure. First, critical potentials, E_- and E_+ were determined in the symmetrical case where two mercury droplets are equally charged. Two mercury

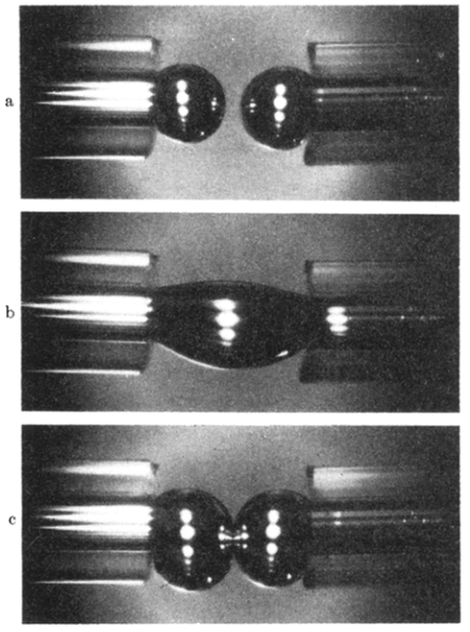

Figure 3. Photographs showing the coalescence and repulsion of mercury droplets: a, growing; b, coalescence; c, repulsion.

droplets were polarized simultaneously by means of potentiometer P_1 against nce after connecting both mercury pools. In the following the polarizing potential E will be given with reference to the rational potential of the electrode; *i.e.*, $E = 0$ when the polarized potential is fixed to the electrocapillary maximum (ecm) potential. The ecm potential (-0.47 v *vs.* nce) was confirmed by measuring the potential at which the differential capacity of mercury in contact with 0.01 *M* KF solution showed a minimum.

If the absolute value of E is small, two droplets coalesce as soon as they grow to the sizes at which their surfaces appear to be in contact with each other. However, if E is increased continuously to the negative or positive direction, a polarization range is obtained over which the twin droplets do not coalesce and continue to grow separately (*i.e.*, repulsion) even if they contact with each other. These behaviors of the mercury droplets were observed *via* the microscope of a cathetometer as shown in Figure 3. After determining the critical potentials, *i.e.*, the upper limit E_+ (>0) and lower limit E_- (<0) of the polarization range of coalescence, the potentiometers P_1 and P_2 were connected as shown in Figure 1a. One of the polarizing potentials, say, E_1 was fixed to any desired value more than E_- or E_+ and then the critical potential of the other side, say E_2, was determined. Below or above the critical potential of E_2 unequally charged mercury droplets coalesced or repelled each other. A set of the

potentials thus obtained provides the critical potential in coalescence of unequally charged mercury droplets (heterocoalescence). Two growing droplets were brought into contact as slowly as possible by regulating three traveling micrometer devices attached to one capillary. It is thought to be necessary to avoid the effect of acting force which results from the nonequilibrium state, such as a resistance in thinning the intervening water layer.[8] In fact, when the contact of the two droplets was not sufficiently slow, the critical potentials showed a tendency to decrease to smaller values. The critical potentials were not so sensitive to the size of the droplets except in the case where the difference in size between the droplets was exceedingly great. The error in the detection of the critical potentials, which depends upon the applied potentials, was estimated to be less than ±6%.

Results and Discussion

Interaction between Identical Double Layers. Critical potentials in the symmetrical case, E_- and E_+, are plotted in Figure 4 as functions of KF concentration in molarity. The symmetry between E_- and E_+ with respect to the abscissa is thought to be satisfactory. The Hamaker constant, A, was evaluated in such a way that a maximum in the net potential energy (V_{max}) became zero at the critical potential under the condition of $\kappa D = 2$ (D is the shortest distance between the particle surfaces, and κ is the Debye–Hückel reciprocal length). The values thus obtained from the critical potentials were $(3.10 \pm 0.19) \times 10^{-12}$ and $(1.20 \pm 0.17) \times 10^{-12}$ at a 5% significant level, respectively, where in the former the surface potential referred to E and in the latter the potential of the outer Helmholtz plane, ψ^0, was used in calculating the double-layer interaction. Though the DLVO theory is originally concerned with the diffuse layer potential, it is thought to be interesting to compare the results from the both calculations. In the above calculations the repulsive potential energy of double-layer interaction was evaluated by interpolating the results established by Devereux and de Bruyn,[4] and $A/12\pi D^2$ [1] was used in estimating the van der Waals attraction. That is, the calculation is based on the plane-parallel double-layer model, but this is thought to be a proper choice for our system.

Conversely, we can calculate the critical potential in each concentration if the value of A is known. The dotted curves in Figure 4 represent the theoretical value of the critical potential in the case of $A = 3.10 \times 10^{-12}$. The solid curves show the theoretical value in the case of $A = 1.20 \times 10^{-12}$ where the double-layer interaction energy was calculated in terms of ψ^0. The agreement between theory and experimental results is thought to be satisfactory in each case. The value of ψ^0 (in volts) in KF solutions was calculated at 25° in accordance with the theoretical equation as

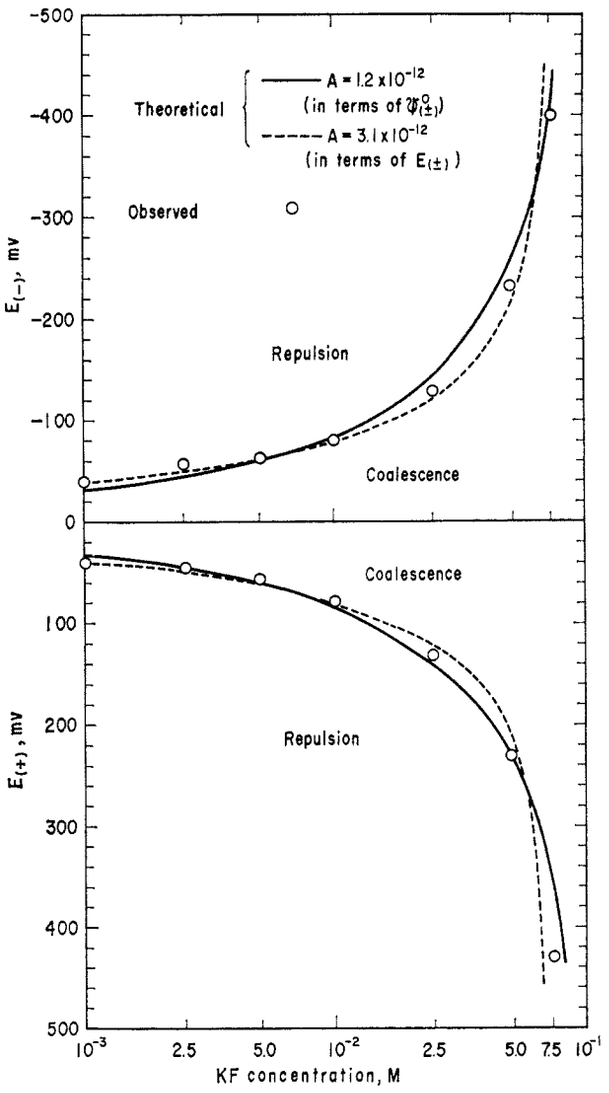

Figure 4. Critical potentials in the symmetrical case as functions of KF concentration.

$$\sigma_S = 11.72C^{1/2} \sinh (19.46\psi^0) \quad (1)$$

where σ_S is the surface charge density in microcoulombs per square centimeter and C is the electrolyte concentration in moles per liter. The surface charge density was obtained by integration of the differential capacity with respect to E except for 0.001 M KF solution. It was difficult in our device to obtain a reliable value of the differential capacity in concentrations less than

(8) B. V. Derjaguin and M. Kussakov, *Acta Physicochim. URSS*, **10**, 25, 154 (1939).

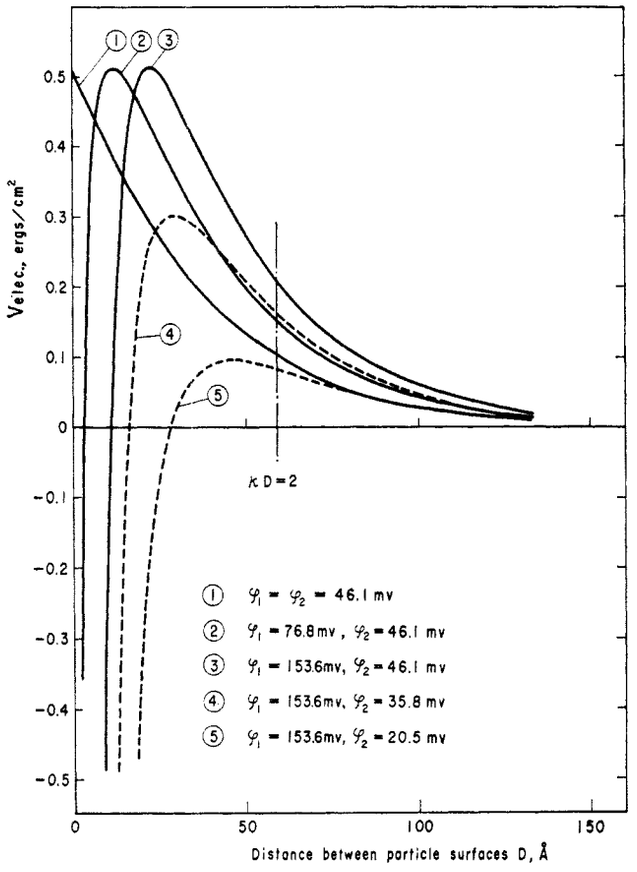

Figure 5. Potential energy due to the double-layer interaction (V_{elec}) as a function of the particle distance in 0.01 M KF solution.

0.0025 M, so that Grahame's data[9] were used for 0.001 M KF solution. The agreement in σ_S between Grahame's and our results was confirmed for 0.01 M and 0.1 M KF solutions. The relation between ψ^0 and E was used for mutual conversion between them.

Interaction between Dissimilar Double Layers in the Absence of Specific Adsorption. Remarkable features demonstrated by Derjaguin[2] are as follows. (a) In contrast to the symmetrical case, a force barrier occurs in the dissimilar double-layer interaction when both potentials are of the same sign. (b) The force barrier depends exclusively on the potential of the more weakly charged surface, say φ_2. (c) The position at which the force barrier appears is shifted to a greater distance as the potential of the more strongly charged surface, say φ_1, increases. The accurate calculation of the potential energy due to the dissimilar double-layer interaction was carried out by Devereux and de Bruyn[4] on the basis of the free energy method. Examples of the potential energy due to the dissimilar double-layer interaction (V_{elec}) in 0.01 M KF solution are illustrated in Figure 5 as functions of the particle distance. Considering that the energy value at $\kappa D = 2$ is a measure of the criterion of the coalescence, it may be seen from this figure that the lower surface potentials, φ_2, must be decreased with increasing higher surface potentials, φ_1, in order to cause the coalescence. The critical potentials determined experimentally in the heterocoalescence are shown in Figure 6. Cross marks along the chain line show the critical potentials (E_- or E_+) in the symmetrical case. The region involving the origin represents the coalescence. In the second and fourth quadrants where two mercury droplets are oppositely charged, the droplets surely coalesce irrespective of the concentration of the solutions under test. In the case of the heterocoalescence, theoretical curves are also given in a way similar to that of the symmetrical case on the assumption that the critical condition corresponds to the point at which $V_{max} = 0$. The Hamaker constant A was evaluated from the experimental value of E_- or E_+ for each concentration. The potential energy due to the dissimilar double-layer interaction was evaluated by a graphical interpolation of Devereux and de Bruyn's table.[4] Solid and dotted curves represent the theoretical values, where the double-layer interaction energies were cal-

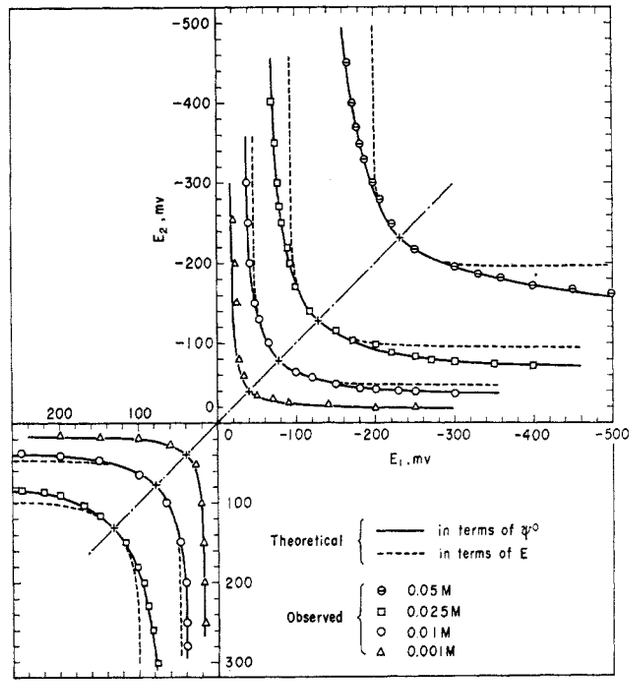

Figure 6. Critical potentials at heterocoalescence in KF solution.

(9) D. C. Grahame, *J. Am. Chem. Soc.*, **76**, 4819 (1954).

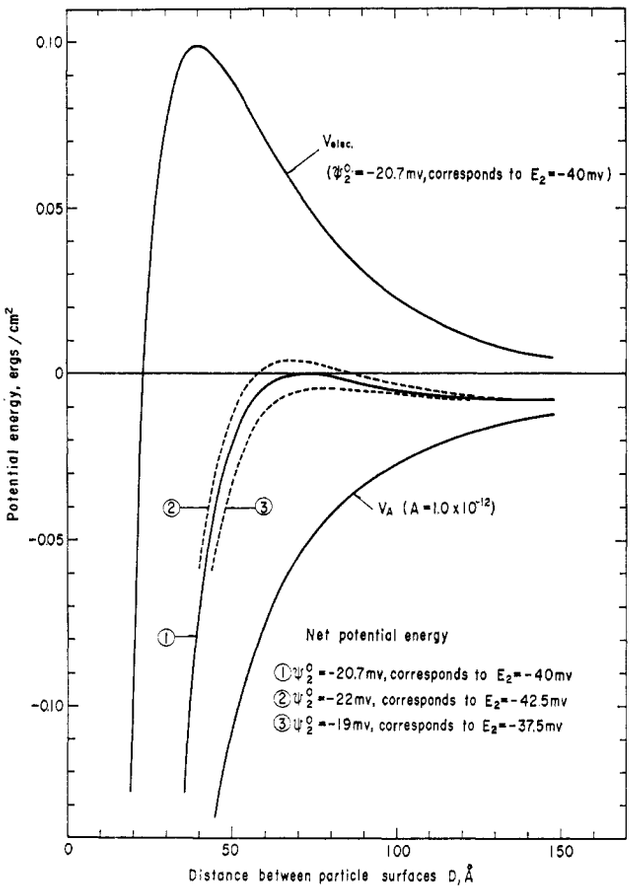

Figure 7. Potential energy curves as functions of the particle distance in 0.01 M KF solution at $\psi^0_1 = -102$ mv (corresponding to $E_1 = -260$ mv).

culated in terms of ψ^0 in the former and in terms of E in the latter, respectively. An example of calculation of the potential energies due to the dissimilar double-layer interaction, V_{elec}, van der Waals attraction, V_A, and total interaction between approaching particles at $\psi_1^0 = -102$ mv (corresponding to $E_1 = -260$ mv) and $\psi_2^0 = -20.7$ mv (corresponding to $E_2 = -40$ mv) is shown in Figure 7 for 0.01 M KF solution. In this figure total potential energy curves at $E_2 = -42.5$ and -37.5 mv are included for comparison. Within the range of these potentials ambiguous results were given to detect the critical potentials.

As is shown in Figure 6, ψ^0 corrections are of significance with higher concentration and less effect appears in dilute solution, especially for 0.001 M solution. The agreement between experimental results and theoretical curves in terms of ψ^0 is thought to be satisfactory. This agreement between theory and experiment proves the validity of the theory of dissimilar double-layer interaction and furthermore indicates that the coalescence of mercury droplets is substantially the same as the coagulation of hydrophobic colloid particles and is interpreted quantitatively by the DLVO theory as has been pointed out by Watanabe and Gotoh.[6] In Figure 4 we obtained the values 3.1×10^{-12} and 1.2×10^{-12} as Hamaker constants, respectively. Confirming the validity of the calculation in terms of ψ^0, it may be concluded that the latter value should be taken as the correct one. This value is very close to the one proposed by Fowkes,[10] 1.3×10^{-12}, which was obtained from a different approach, and this indicates that the interaction between mercury and water molecules consists mainly of molecular forces, because he obtained the value by assuming that the interaction between mercury and water is composed entirely of the London–van der Waals forces and no contribution from electrostatic origin is expected. This may be the reason why the *coalescence* of mercury droplets in water was well interpreted in terms of the *coagulation* theory of hydrophobic colloids.

Interaction between Dissimilar Double Layers in the Presence of Specific Adsorption of Anions. Similar experiments were made on the aqueous solutions of KI with an intention of checking the effect of the specific adsorption of I^- ions. In contrast to KF solutions, no coalescence was observed in 0.001, 0.01, and 0.025 M KI solutions in the whole range of the potential tested. It should be noted that the mercury droplets repel each

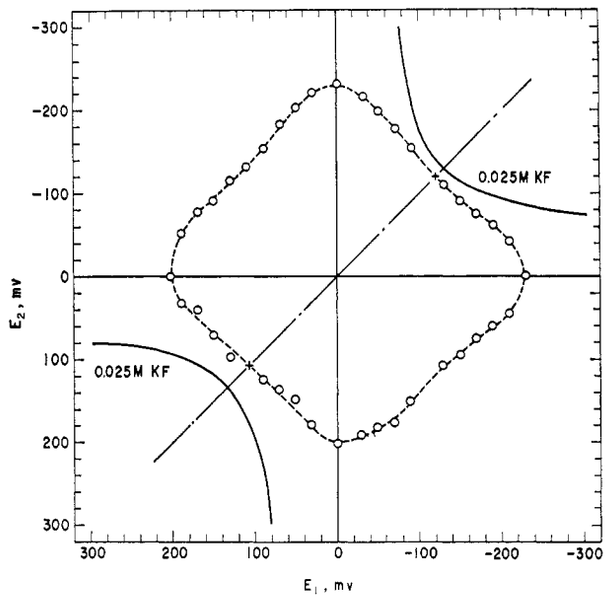

Figure 8. Critical potentials at heterocoalescence in the solution of KI + KF of constant ionic strength, 2.5×10^{-2} M. The concentration of KI is 1×10^{-4} M.

(10) F. M. Fowkes, *Ind. Eng. Chem.*, **56**, 40 (1964).

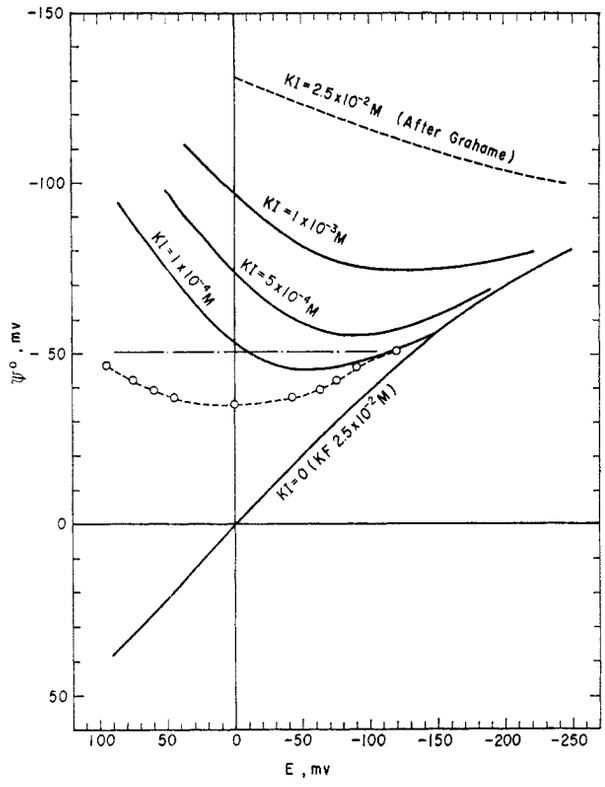

Figure 9. Relation between ψ^0 and E in the solution of KI + KF of constant ionic strength, 2.5×10^{-2} M: --O--, calculated from the coalescence data for [KI] = 1×10^{-4} M.

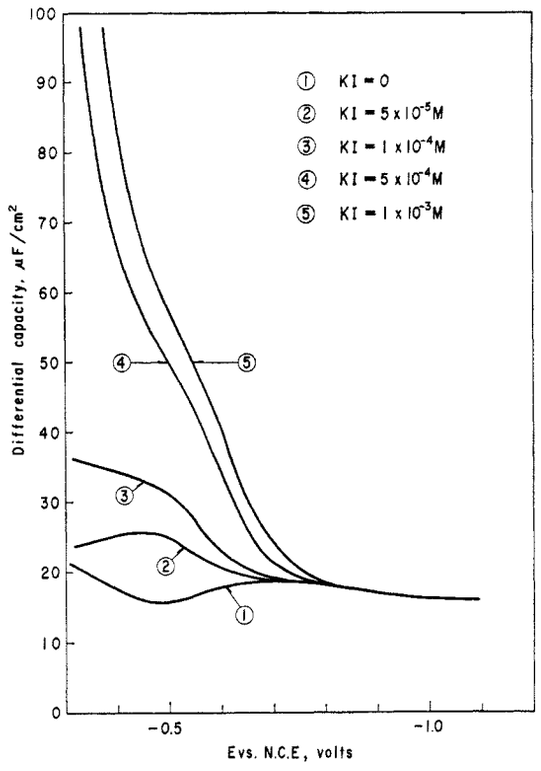

Figure 10. Differential capacities of mercury in contact with the solution of KI + KF of constant ionic strength, 2.5×10^{-2} M.

other even if they are oppositely charged. This fact may be interpreted by assuming that the potential of the outer Helmholtz plane, ψ^0, becomes negative as a result of the specific adsorption of I^- ions, even though the potential of the mercury surface, E, is fixed to the positive side. In order to examine quantitatively the effect of ψ^0 on the coalescence of mercury droplets in the presence of KI, the experiments were undertaken with the solution of KI + KF of constant ionic strength, 2.5×10^{-2} M. In the solutions where [KI] = 5×10^{-5}, 1×10^{-4}, 5×10^{-4}, and 1×10^{-3} M, the coalescence took place only in the first two solutions. In this case, however, the pattern of the critical potentials in the heterocoalescence differs considerably from that in the case of the pure KF solutions. In Figure 8, the critical potentials were plotted for [KI] = 1×10^{-4} M, the range including the origin representing the coalescence. In the same figure the result for the pure KF solution (2.5×10^{-2} M) was included for comparison. From these results we can estimate the ψ^0 for this system as a function of E with the aid of the critical potential data for the pure KF solution of 2.5×10^{-2} M, if we assume that the coalescence of mercury droplets is predominantly determined by ψ^0. In the above calculation it was reasonable to consider from the differential capacity data that the ψ^0 in the range more negative than $E = -150$ mv does not differ from that of the pure KF solution (2.5×10^{-2} M). The results for KI = 1×10^{-4} M are shown in Figure 9 as circles with a dotted line. Solid curves in the figure show the value of ψ^0 calculated from the differential capacity data. Differential capacities as functions of the potential against nce is illustrated in Figure 10. ψ^0 can be calculated by use of the eq 1, but in this case σ_S must be replaced by $\sigma_S + \sigma_{I^-}$ (σ_{I^-} is the amount of specifically adsorbed I^- ions). For our system, σ_{I^-} is obtained by the relation[11]

$$F(\partial\gamma/RT\partial \ln m_{KI})_{Ence} = -\sigma_{I^-} \quad (2)$$

where F is the faraday, γ is the interfacial tension, and m_{KI} is the molal concentration of KI. The value of γ (relative to ecm) was obtained by double integration of the capacity values with respect to E. As is seen in Figure 9, a poor agreement is noted between both approaches for 1×10^{-4} M KI and the discrepancy is much pronounced as the potential becomes positive.

(11) E. Dutkiewicz and R. Parsons, *J. Electroanal. Chem.*, 11, 100 (1966).

A series of measurements of differential capacity at different frequencies (100, 300, 1000, and 3000 cps) was made, and a dependence on the frequency was observed at potentials more positive than −0.7 v (*vs.* nce). Consequently, the above calculation was also carried out by using the differential capacity values extrapolated to zero frequency, but the discrepancy was not diminished at all. The reasonable explanation for this has not yet been given. However, the results in Figure 9 account qualitatively for the behavior of coalescence and repulsion of mercury droplets in KI solution. From the results that the critical potential ψ^0_- in the symmetrical case was −50.5 mv (corresponding to $E_- = -128$ mv), which is marked by the horizontal chain line, for the pure KF solution of 0.025 M (in the absence of specific adsorption), it may be expected that no coalescence takes place at any potential E in the KI solutions more concentrated than 5×10^{-4} M and coalescence occurs in the KI solutions less dilute than 1×10^{-4} M. This expectation is supported by the experimental results as previously described. Thus, the qualitative interpretation of the coalescence of mercury droplets in the presence of specific adsorption of I^- ions is possible in terms of the potential of the outer Helmholtz plane at the mercury–solution interface.

Acknowledgment. This investigation was supported in part by a Grant-in-Aid for Cooperate Research from the Ministry of Education. We are grateful to Professor Akira Watanabe of Kyoto Technical University for his valuable discussions and to Assistant Professor Tsuneo Ikegami of the Chemical Research Institute of Non-Aqueous Solutions of Tohoku University for his help with assembling our devices.

Infrared Spectrum of AlF_3, Al_2F_6, and AlF by Matrix Isolation

by Alan Snelson

IIT Research Institute, Chicago, Illinois 60616 *(Received February 14, 1967)*

The matrix isolation technique has been used to obtain the infrared spectrum of AlF_3, Al_2F_6, and AlF. Orientation effects observed for AlF_3 trapped in an argon matrix aided in the assignment of some absorption bands. The following are the three infrared-active frequencies of AlF_3: $\nu_4(E')$ 270 cm^{-1}, $\nu_3(E')$ 965 cm^{-1}, and $\nu_2(A_2'')$ 300 cm^{-1}. Six frequencies are attributed to the dimer Al_2F_6. Assuming a planar bridge structure, point group D_{2h}, the frequencies are assigned as follows: $\nu_8(B_{1u})$ 995 cm^{-1}, $\nu_9(B_{1u})$ 340 cm^{-1}, $\nu_{13}(B_{2u})$ 660 cm^{-1}, $\nu_{16}(B_{3u})$ 805 cm^{-1}, $\nu_{17}(B_{3u})$ 575 cm^{-1}, $\nu_{18}(B_{3u})$ 300 cm^{-1}.

Introduction

Mass spectroscopic investigations[1,2] have shown aluminum trifluoride vapor at about 1000°K to consist of the molecular species AlF_3 and Al_2F_6, the latter being present to the extent of 1 or 2%. The high-temperature gas-phase infrared spectrum of AlF_3 has been reported by Buchler[3] and Margrave, *et al.*[4] The matrix spectrum has been observed by Linevsky[5] and Snelson[6] but is not reported in the open literature. No data are available on the dimer species. The current investigation by matrix isolation was initiated to fill

(1) R. F. Porter and E. E. Zeller, *J. Chem. Phys.*, **33**, 858 (1960).

(2) A. Buchler, "Study of High Temperature Thermodynamics of Light Metal Compounds," Progress Report No. 3, Arthur D. Little, Inc., Cambridge, Mass., 1962.

(3) A. Buchler, ref 2, Progress Report No. 2.

(4) L. D. McCory, R. C. Paul, and J. L. Margrave, *J. Phys. Chem.*, **67**, 1986 (1963).